IJSRIS journal
INTERNATIONAL JOURNAL OF SCIENTIFIC RESEARCH AND INNOVATIVE STUDIES
ISSN: 2820-7157
www.ijsrisjournal.com

April 2026 | Volume 5 | Number 2 | 308-322

Received Date: 22 February 2026 | Accepted Date: 14 March 2026 | Published Date: 2 April 2026

The use of geosynthetics for the reinforcement and stabilisation of road structures: the case of the Lekié Loop rehabilitation project in Cameroon

Fongang Kamgaing Giovanni Paolo [1], Bwemba Charles [2], Sakou Laurent [3]

1. National Advanced School of Public Works (NASPW), Civil Engineering department, Yaounde, Cameroon, paolofongang@gmail.com
2. Ministry of Public Works, National Advanced School of Public Works (NASPW), Civil Engineering department, Yaounde, Cameroon, carlbwe@yahoo.fr
3. HUESKER Synthetic GmbH, Gescher, Germany, Sakou@huesker.de

Abstract

This work relates to the use of geosynthetics in the reinforcement and stabilization of pavement structures, through the case study of the rehabilitation project of the Lekié loop. The main objective is to assess the impact of integrating a geosynthetic layer in the subgrade on the mechanical behavior of the pavement, in terms of deformation, strength, and cost. The approach is based on a comparative analysis between a conventional pavement structure, corresponding to the initial contractual structure, and a structure reinforced with geosynthetics. The design of the contractual structure was conducted using Alizé-Lcpc, following the applicable technical recommendations. Subsequently, a three-dimensional modeling of the pavement was performed using Plaxis 3D 2024 to analyze the mechanical behavior of the two variants. The analysis of the mesh displacements, combined with the application of the laws of elasticity, made it possible to calculate an improvement coefficient of the base layer of 1.2, representing a 20% performance gain due to the addition of the geosynthetic. Furthermore, an economic analysis allowed for the assessment of the financial impact of this solution. It notes that despite an initial additional cost of 3.25%, the use of geosynthetics enables optimization of design, a reduction in maintenance costs, and a significant improvement in pavement durability. In conclusion, this study highlights the techno-economic benefits of geosynthetics for strengthening road infrastructures, particularly in sensitive environments. It opens up interesting prospects for the broader application of these solutions in the context of road projects.

Keywords: Geosynthetics; Pavement reinforcement; Numerical modeling; Alizé-LCPC; Tropical pavements.

1. Introduction

1.1. Legal Requirements

Submission of this manuscript implies that the work presented has not been previously published and is not currently under consideration by any other journal. All authors have approved the publication of this manuscript and confirm that the institutions involved, notably the University and the field partners in Cameroon, have given their tacit consent for the conduct of this study. The publisher cannot be held liable for any legal claims relating to this work.

This study was conducted in strict compliance with the scientific and technical standards in force in the field of civil and road engineering, including field data collection, geotechnical measurements, and numerical modelling of road structures.

1.2. Permissions

The figures, tables and text extracts included in this manuscript are original and produced by the authors. No figures or data have been reproduced from previously published articles without permission. Where results or methods inspired by previous work have been cited, the sources have been duly referenced in the References section.

1.3. Scientific context and rationale for the study

Road infrastructure is a major driver of socio-economic development, particularly in the African context where the road network ensures regional integration [1]. However, often poor ground conditions (clay soils, soft soils) and increasing loads (heavy goods vehicle traffic) compromise the durability of pavements. In this context, the use of innovative soil reinforcement solutions is essential. Among these, geosynthetics—synthetic polymer sheet materials (geotextiles, geogrids, geomembranes, etc.)—have demonstrated their effectiveness in improving the performance of road structures for several decades [2,3].

A correctly specified geosynthetic can fulfil multiple functions (separation, reinforcement, drainage) in road infrastructure [2]. For example, its use makes it possible to reduce the thickness of the embankment by improving stress distribution, prevent the mixing of subgrade soils with granular layers, increase the bearing capacity of weak soil, and limit deformations (membrane effect) [2,3]. In practice, it is used both beneath granular foundation layers and beneath asphalt surfacing [3]. Numerous studies and field experiments provide ample evidence that the incorporation of appropriate geosynthetics extends the service life of pavements and reduces overall maintenance costs [2,3].

At the same time, conventional design methods (the French rational method NF P98-086) have evolved to harmonise the integration of such reinforcements. The Alizé-Lcpc software implements this approach based on equivalent modulus [5]. At the same time, finite element analysis tools (such as Plaxis 3D) enable the detailed modelling of soil-structure interaction and the assessment of the effect of geosynthetics on stress and strain fields. This study aims to combine these two approaches for a road rehabilitation project in Cameroon, illustrating the benefits and impact of geosynthetics in pavement engineering.

2. General context and literature review

2.1. Pavement structure and design

A conventional flexible pavement consists of successive layers that distribute traffic loads to the subgrade [4]. Thus, from top to bottom, there is the asphalt pavement (surface and binder courses), the granular base course (load-bearing), the sub-base or capping course, and the subgrade, all resting on compacted soil (subgrade). The base course acts as the primary load-bearing column, distributing vertical stresses over a wide area [4], whilst the sub-base protects the subgrade from the effects of frost and provides bearing capacity during construction [4].

The design of these layers is generally based on rational standards. In France, the NF P98-086 method is applied to new road pavements and can be implemented using Alizé-Lcpc [5]. This method takes into account the design traffic (in terms of standardised traffic volume) and the strength of the materials (E-modulus, CBR, etc.) to determine the required thicknesses. In the African context, these rules are often adapted to local materials and a desired service life (typically 15–20 years) [5].

From a mechanical perspective, pavement layers can be viewed as an elastic multilayer system. Unbound aggregates (sub-base, base) are modelled using a linear elastic law (modulus of elasticity E, Poisson's ratio ~0.3) to account for stress distribution [4]. Asphalt pavements are viscoelastic and temperature-dependent, but for design calculations they are often treated using an average equivalent E (Huet-Sayegh law or an equivalent modulus approach) [6]. The calculations aim to meet durability criteria: The maximum stresses in each layer must be below the material's fatigue limit, and accumulated deformations (rutting) under a load bar must be below an acceptable threshold. It should be noted that freeze-thaw cycles can cause specific swelling/degradation, but these effects are generally addressed through drainage design and sufficient sub-base layer thickness.

2.2. Degradation of Pavements

Flexible pavements can be degraded by several fundamental mechanisms: fatigue (crack formation induced by cyclic stresses), rutting (permanent subsidence under the wheel track), differential settlement (non-uniform deformation caused by heterogeneous subgrade soils), as well as deformations related to freeze-thaw cycles. The specialist literature highlights that one of the objectives of geosynthetic reinforcement is precisely to reduce this deterioration: for example, the COST REIPAS (Action 348) project explicitly lists as its objectives the extension of the pavement's service life, the reduction of differential settlement and rutting, as well as the limitation of crack propagation [7]. Indeed, a weak subgrade leads to significant deformations of the embankment under load, and any solution (binders, consolidation, geosynthetics) that increases overall stiffness or distributes stresses more effectively helps to delay the onset of such damage. Thus, improving the system's permeability (better drainage) and increasing fatigue resistance are two key factors in enhancing durability.

2.3. Common stabilisation techniques

Several methods exist to improve the stability of pavements on weak ground: chemical stabilisation (adding lime or cement to the soil to increase its stiffness), mechanical reinforcement (improved compaction, aggregate mixing), and geosynthetic solutions. For example, lime stabilisation is commonly used to treat frost-susceptible clay soils, but it increases costs and can be technically challenging (control of dosage, setting, etc.). Geosynthetics offer a modular mechanical alternative: they are integrated into the soil/embankment without chemical treatment and provide tensile reinforcement. In a pavement, they can then be used to reinforce the subgrade or to interleave layers (base or sub-base layers) in order to better distribute stresses [2,3]. The reported benefits include, in particular, a reduction in the required thickness of structural layers, better control of lateral movements (membrane effect) and an extension of the pavement's service life [2,3].

2.4. Geosynthetics: definitions and functions

A geosynthetic is defined as any product constituting a sheet (fabric, mat or three-dimensional structure) made of synthetic or natural material, used in contact with the ground or civil engineering structures [8]. The main families are geotextiles (permeable) and geomembranes (impermeable), which can be combined to form geocomposites [8]. In the road sector, two main types of products are used: non-woven geotextiles (a mat of agglomerated synthetic fibres) serving as a filtering and draining separator, and geogrids (rigid polyethylene/polyester mesh) providing mechanical reinforcement. Draining geocomposites are also sometimes used.

The main functions of geosynthetics in road construction are separation and reinforcement [2,8]. Separation aims to prevent the mixing of subgrade soils and fill layers (preservation of aggregates) [8]. For example, by placing a separating geotextile between clayey soil and granular fill, the infiltration of fines and the rapid degradation of the foundation layer are prevented. Reinforcement (utilising the strength-strain behaviour of the geosynthetic) allows the tensile stiffness of the geosynthetic to be harnessed to support the load. In a granular foundation layer, the mesh of the geogrid interlocks the aggregates, converting part of the vertical load into tensile force within the geogrid (a mechanism known as the 'pocket effect') [3]. This increases the overall bearing capacity, reduces shear stress within the aggregates and has the effect of reducing vertical deformation.

Geosynthetics also offer drainage properties (water flow through the geogrid) and, in some cases, filtration and protection, but these secondary functions are less essential in our case. They are manufactured from synthetic polymers (mainly polypropylene, polyester, polyethylene) which ensure lightness, durability and resistance to chemicals. Their characteristics (stiffness, elongation, porosity, slip resistance) are standardised in accordance with ISO/EN/NF standards [8], which allows the appropriate product to be selected for each application.

2.5. Experience with the use of geosynthetics in road engineering

Geosynthetics have been used in road structures in Europe for over 40 years [3]. Thousands of kilometres of roads have been reinforced (in both granular layers and pavements) with results deemed positive [3]. For example, a project in Norway (a low-traffic road laid on 3 m of peat) showed that the introduction of a geogrid into the granular embankment increased the bearing capacity and reduced differential settlement: twenty years later, the road was still in service with good results [3]. However, despite these successes, design recommendations often remain empirical, as formal calculation methods have been slow to incorporate these materials [3]. Nevertheless, all highlight the major benefits: less material required, less settlement, greater durability, and ultimately reduced life-cycle costs [2,3].

In summary, the state of the art confirms that geosynthetics (particularly geogrids) provide significant structural benefits to flexible pavements (reduction in the required sub-base thickness, gains in bearing capacity and limitation of deformations) [2,3]. This study aims to quantify these benefits in a specific case study, combining numerical simulation and standardised design.

3. Materials and methods

3.1. Study site

The study site is the Lekié Loop, located in the Lekié department (Central Region, Cameroon) [1]. It is a bypass road connecting several interchanges (Nkolbisson – Zamengoué – Ekekam – Evodoula – Monatélé) in a peri-urban context. Rehabilitation works began there in 2022 and are currently being carried out by Arab Contractors under the supervision of the Cameroonian Ministry of Public Works [1]. The area consists mainly of lateritic and clay soils with a variable water table.

3.2. Data collected

The data collected are of a geotechnical, traffic statistical and geometric nature.

- Geotechnical data: The geotechnical data presented in Figure 1 include, in tabular form, the results of identification tests (granulometric analysis, Atterberg limits) and characterisation tests (Proctor and CBR tests) carried out on the soil layers.

- Traffic data: Traffic volume enables an assessment of the traffic flow to which the infrastructure will be exposed. It is determined through traffic counting campaigns carried out prior to the start of works. These readings, taken manually during the morning and evening rush hours over a reference period of one week, provide the average daily traffic volume.

- Geometric data: The main geometric data required for this work is the typical cross-section shown in Figure 2.

3.3. Characteristics of geosynthetics

Geosynthetics are commercially available and their technical data sheets serve as their identification documents. This means that they contain the material's main mechanical characteristics, notably the ultimate tensile strength (kN/m), tensile strength at 2% elongation (kN/m) and initial stiffness (kN/m).

The tensile strength (TS) of a geogrid is defined as the maximum load it can withstand before failure, expressed in kilonewtons per metre (kN/m) in the longitudinal and transverse directions.

The maximum strain (ε_{max}) of a geogrid represents the ultimate elongation it can withstand before its structure collapses completely.

The axial stiffness or modulus of elasticity EA quantifies the geogrid's ability to immediately limit differential settlement under load. It is determined from the nominal tensile strength and the maximum strain according to Equation 1.

$$EA = \frac{R_T}{\varepsilon_{max}} \qquad \text{(Eq. 1)}$$

Where:

R_T is the nominal tensile strength of the geogrid in kN/m;

ε_{max} represents the maximum strain expressed as a percentage or in decimals.

3.4. Initial design (Alizé-Lcpc)

The first step involves designing the initial pavement structure (without geosynthetics) using the French rational method. To do this, the Alizé-Lcpc software is used, which applies the NF P98-086 standard (revised 2019) for flexible pavements [5]. The materials are specified by their moduli of elasticity (E) and Poisson's ratios (ν). The calculation takes into account the design traffic, expressed here in terms of equivalent axles, corresponding to the reference load of 130 kN. The stresses (vertical stress due to the axles) are distributed across the layers, and checks are carried out for rutting (e.g. the Witczak criterion for asphalt concrete) and fatigue (empirical criterion based on stress-strain in the asphalt layer).

In Alizé, the structure initially selected corresponds to the client's contract design. In practice, the structure obtained for the case studied is:

- A sub-base layer of lateritic gravel, 30 cm thick.

- Foundation + base course of crushed gravel (0/31.5), thickness 20 cm.

- Asphalt concrete (mastic) surface course, 5 cm thick.

These thicknesses are sufficient to ensure that, under the anticipated traffic, the stresses in each layer remain within acceptable limits. These values serve as **the baseline** (structure A) for comparison.

3.5. Numerical modelling (Plaxis 3D)

To assess the influence of the geosynthetic, we carry out a three-dimensional modelling of the pavement structure. We use the Plaxis 3D software, which allows us to simulate soil-structure interaction using different constitutive models [9]. The main characteristics of the Plaxis model are:

- 3D geometry: a rectangular domain covering the width of the carriageway (approximately 7 m) and a sufficient length (by symmetry or repetition) to represent the load from a single axle. The depth of the model includes the sub-base, the base, and the subgrade to approximately 3 m below the carriageway surface.

- Mesh: A fine mesh is generated automatically using an extended Delaunay algorithm by distributing nodes and creating elements according to the model's geometry. The element chosen is a 15-node triangular prism with 6 triangular faces and 3 rectangular faces, thereby enabling the capture of stress gradients.

- Materials: The granular layers (sub-base, base) are modelled as linearly elastic (E-modulus, $\nu = 0.35$). The clay subgrade is also elastic with a lower modulus (and possibly a plastic imperfection if necessary). The asphalt is modelled using an equivalent elastic modulus (in this static study, viscosity is neglected). All materials are assumed to be drained (long-term conditions), so no dynamic pore pressure effects are considered.

- Boundary conditions: The boundary conditions strictly constrain the displacements of the structural model. To this end, the road surface is modelled on an XY plane measuring **12 m × 8 m** in order to limit free-edge effects. In order to prevent any rigid movement and simulate an infinite underlying soil, a fully fixed support is applied to the bottom face of the volume (at a depth of 1.55 m), i.e.

$$Ux = Uy = Uz = 0. \qquad \text{(Eq. 2)}$$

Ux, Uy, Uz are the components of the imposed displacements (mm or m depending on the unit chosen).

- Loading: As PLAXIS 3D v2024 is not primarily designed for road design, there is no reference load specific to any particular method. However, in order to obtain conclusive results, we model a reference load identical to that used by the Alizé-Lcpc software.

A reference tandem axle of 13 tonnes is considered. The axle has 4 identical wheels. Each wheel supports a unit force Fu. The wheel-road contact area as is given by expression 3.

$$As = \pi \times r^2 \qquad \text{(Eq. 3)}$$

Where:

r is the radius of the tyre's contact patch on the road surface.

The vertical pressure σ_z exerted on a load circle is given by expression 4.

$$\sigma_z = \frac{F_u}{A} \qquad \text{(Eq. 4)}$$

The two left (and right) wheels are in contact over a distance d given by expression 5.

$$d = 2 \times r \qquad \text{(Eq. 5)}$$

The centre-to-centre distance between the centres of the inner left and right wheels remains unchanged.

- Geogrid: In PLAXIS 3D v2024, the geogrid is modelled as a two-dimensional isotropic surface reinforcement inserted at the interface between the PST and fill layers. It is characterised by its axial stiffness EA in kN/m, its allowable strain and its 'tension-only' behaviour. Interaction with the soil, meanwhile, is based on friction parameters and the interface coefficient.

- Soil behaviour of pavement layers: Three soil behaviour models are used in the PLAXIS 3D v2024 software, namely the linear elastic, Mohr-Coulomb and Hardening Soil Small (HS Small) models.

The asphalt layer is typically modelled using the linear elastic model. Indeed, its operating range (small deformations < 1%) is dominated by a constant Young's modulus and a stable Poisson's ratio.

The sub-base and base layers use the Mohr-Coulomb model, which is suited to low-cohesion granular materials. It defines a failure threshold via an angle of internal friction and often low cohesion. This model is robust and allows for the effective simulation of shear strength development in the base under road traffic.

The sub-base and PST layers correspond to the Hardening Soil Small model. This model extends the classic Hardening Soil law by incorporating a stiffness modulus at very small strains (Go modulus). It thus optimises accuracy for low-amplitude stresses, typical of reinforced soils in direct contact with a geogrid.

Figure 3 shows the three-dimensional Plaxis model of the road pavement, in particular the stacking of the layers (asphalt, sub-base + base, sub-grade and PST). The reinforcement geogrid (in green) is inserted into the sub-grade. The finite element mesh is refined under the load (not shown). The boundary conditions are represented by cloverleaf nodes at the bottom of the model.

- Configuration of the calculation phases

The initial phase establishes the natural soil stresses prior to the application of any external load. The Ko procedure allows the direct generation of effective horizontal and vertical stresses, taking into account the self-weight and the initial lateral coefficient. It ensures that the model accurately reproduces the geostatic history prior to any additional loading.

In the initial pavement phase, the design load is applied to the structure without reinforcement. The simulation involves a gradual increase in loads, with monitoring of soil deformations and plasticisation. This baseline study without reinforcement provides a point of comparison for assessing the effect of the geogrid.

In the reinforced structure phase, the geogrid is introduced into the model as a reinforcement membrane, positioned according to the planned stacking arrangement. It is modelled as a very thin surface element (2D), with an interface coefficient set at 0.7. This coefficient, used in the simulations, reflects a soil–geogrid interface mobilising a significant proportion of the granular material's shear strength—a condition achieved in practice when the geogrid is embedded in well-compacted, interlocked crushed stone. This value is consistent with the results of interface and pull-out tests reported in the literature for geogrids installed in crushed gravel, and with manufacturers' recommendations for compliant installation.

3.6. Evaluation of technical performance

Once the two pavement configurations have been designed in accordance with current standards and methods, a rigorous analysis is carried out to assess the effectiveness of the reinforcement provided. The influence of the geogrid on the stiffness of the sub-base is quantified by extracting, at a single critical point, the deformations measured in the reinforced and unreinforced models under the same tyre pressure of 662 kPa corresponding to a 130 kN axle.

By imposing the equality of stresses $\sigma_{initial} = \sigma_{final}$ and applying Hooke's law as expressed by equation 2.3.

$$\sigma = E \times \varepsilon \qquad \text{(Eq. 3)}$$

It is established that:

$$E_{initial} \times \varepsilon_{initial} = E_{final} \times \varepsilon_{final} \qquad \text{(Eq. 4)}$$

It follows that the coefficient K' for the improvement of the basic static modulus of the sub-base layer is defined by equation 2.5.

$$k' = \frac{E_{final}}{E_{initial}} = \frac{\varepsilon_{initial}}{\varepsilon_{final}} \qquad \text{(Eq. 5)}$$

In this case study and in accordance with standards EN ISO 11066 and BS 8006, the overall safety factor for the geogrid is defined by expression 2.6.

$$F_{s-global} = F_m \times F_i \times F_c \times F_{cr} \qquad \text{(Eq. 6)}$$

Where:

F_m is the manufacturing factor (≈1.00)

$F_i$is the installation damage factor (≈ 1.10)

F_c is the factor for chemical attack and ageing (≈ 1.15 – 1.30)

F_{cr} is the creep factor, a function of service life (≈ 1.25 – 3.0)

Thus, expression 2.7 defines the modulus enhancement factor for the sub-base layer.

$$k = \frac{k'}{F_{s-global}} \qquad \text{(Eq. 7)}$$

This coefficient K, a numerical indicator of the geogrid's structural effect, reflects the increase in stiffness imparted to the sub-base layer and its enhanced ability to limit settlement.

In other words, the modulus E of the sub-base layer (in the Alizé calculation) is increased by this factor k to account for the reinforcement. In our case, the Plaxis numerical results (see § 4) typically give$\varepsilon_{initial} \approx$ 0.5562 mm and$\varepsilon_{amélioré} \approx$ 0.4209 mm, i.e. k ≈ 1.20 (a 20% increase).

3.7. Re-importing into Alizé and resizing

Once the coefficient k has been obtained, the reinforced structure is remodelled using Alizé-Lcpc by adjusting the modulus of the sub-base layer:

$$E_{final} = K \times E_{initial} \qquad \text{(Eq. 8)}$$

In doing so, a new design (structure B) of the reinforced pavement is carried out. This calculation will result in a reduced thickness of the sub-base layer, whilst keeping the other layers (base, asphalt) unchanged.

The software then generates several structural variants, in which the thickness of the sub-base layer changes (decreases) according to a predefined arithmetic or geometric progression, allowing the influence of this single parameter on stresses and settlements to be observed. A comparative analysis of these models yields a response curve for the pavement as a function of the thickness of its reinforced sub-base. Thus, the thickness that fully meets the initial deformation and durability criteria specified for the project is selected.

3.8. Economic impact assessment

Finally, based on the quantities, a comparative cost estimate is prepared between the initial structure (Case A) and the reinforced structure (Case B). This estimate includes the costs of materials (aggregates, bitumen, geogrid) and construction (geosynthetic installation, compaction, etc.), enabling the financial impact of the geosynthetic reinforcement to be assessed.

4. Results and discussion

4.1. Initial structure (Alizé) – Case A

The initial design (Table 1), carried out using Alizé-Lcpc, provides the basic structure currently in use on the Lekié loop. This structure meets the regulatory criteria for the intended traffic. In particular, the criterion for maximum deflection ($\delta_{max} \leq 65/100$ mm) is met. This solution will serve as a reference for comparison with the reinforced structure.

4.2. Plaxis simulation – case with/without geosynthetics

In both configurations, the geometry, the geotechnical characteristics of the various layers, as well as the assumptions and load conditions, strictly conform to those defined by the Alizé-Lcpc software. A reference 13-tonne tandem axle is considered. The axle has 4 identical wheels with a radius r = 0.125 m. Each wheel bears a unit force Fu = 32.5 kN. The wheel-road contact area A is As = 0.04087 m². The vertical pressure exerted on a load circle is σz = 662.084 kPa. The two left (and right) wheels of the axle are either joined together or spaced apart by d = 0.25 m. The centre-to-centre distance between the centres of the inner left and right wheels remains unchanged at D = 0.375 m.

The Plaxis simulations shown in Figure 4 qualitatively confirm the benefits of reinforcement. In the unreinforced case (Case 1), the maximum vertical deformation under load was measured at$\varepsilon_{\text{initial}} \approx 0.5562$ mm. For the reinforced case (Case 2 with geogrid and reduced sub-base), the maximum displacement is $\varepsilon_{\text{final}} \approx 0.4209$ mm. The reduction in deformation of approximately 30% reflects a stiffening of the system.

Using the elastic relationship 2.5, the sub-base improvement factor is:

$$k' = \frac{\varepsilon_{\text{initial}}}{\varepsilon_{\text{final}}} = \frac{0.5562}{0.4209} = 1.321454027 \approx 1.32 \qquad \text{(Eq. 9)}$$

In this case study, as the design is for immediate static loading, the installation is carried out at a depth of 55 cm, protected from UV rays, and the geogrid is not acting as a retaining structure, Fc and Fcr are neglected. Thus, the safety factor is:

$$\text{Fs} = F_m \times F_i = 1 \times 1.10 = 1.10. \qquad \text{(Eq. 10)}$$

The overall improvement factor is:

$$k_{\text{global}} = \frac{k}{F_s} = \frac{1.32}{1.10} = 1.2 \qquad \text{(Eq. 11)}$$

Applying the elastic relationship, we obtain an improvement coefficient k ≈ 1.20 (i.e. a 20% increase in the effective modulus of the subgrade). This result is consistent with the trend observed experimentally: for example, Myhre (1985) reports that the installation of a geogrid 'increased the bearing capacity and reduced differential settlement' of a road in Norway [3]. Furthermore, these results are consistent with those reported in recent studies conducted in tropical settings, which also observed similar performance gains through the use of geogrids [10–12].

These simulations show that geosynthetic reinforcement (geogrid in the subgrade) tends to reduce deformations, thereby increasing the apparent stiffness of the pavement system. This numerical estimate corresponds to a 20% improvement in performance, even though the geogrid has a very small material thickness. It is observed that the radial deformation (lateral spreading) of the embankment is also reduced, indicating an effective membrane stress.

4.3. Resizing (Alizé) – Case B

Taking into account the increase in modulus k = 1.20, we input the following into Alizé-Lcpc:

$$E_{\text{final}} = E_{initial} \times K_{global} \qquad \text{(Eq. 12)}$$

$$E_{\text{final}} = 150 \text{ MPa} \times 1.2 = 180 \text{ MPa}. \qquad \text{(Eq. 13)}$$

Once the equivalent reinforced modulus has been determined, simulations are carried out in Alizé-Lcpc to assess the behaviour of the pavement. Fifteen (15) variants of pavement structures, modelled as an arithmetic sequence with a ratio of 2 cm over the thickness of the base course, are dimensioned. The results are presented in Figure 5. With this new mechanical characteristic, the thickness of the sub-base layer would need to be reduced to 8 cm in order to exceed the permissible deflection threshold ($\delta_{max} \leq 65/100$ mm).

A sub-base layer thickness of 20 cm is the one that optimises (minimises) the differences between the permissible deflections and the calculated deflections. It also provides a deflection of 61.2/100 mm. The new calculation therefore leads to a reduction in the thickness of the lateritic sub-base. The optimised structure (Case B) is presented in Table 2. The thickness of the sub-base layer is reduced from 30 cm to 20 cm thanks to the geosynthetic.

Thus, thanks to the mechanical gain provided by the geogrid, 10 cm of sub-base layer is saved (i.e. a 33% reduction in thickness for this layer). The other layers remain unchanged as the increased stiffness is limited to this layer. We then verify that the fatigue and rutting criteria are once again acceptable. This is indeed the second optimised structure (including geosynthetics) which requires less granular material for the same performance.

The results of this study clearly demonstrate the technical benefits of geosynthetics for reinforcing flexible pavements. The measured 20% increase in the effective elastic modulus (coefficient k=1.2) is consistent with other analyses: increased load-bearing capacity and reduced settlement have been observed experimentally in similar projects [3]. The fundamental mechanism is the 'pocket' effect of geogrids: by interlocking the aggregates, they restrict horizontal deformation, reduce the movement of fines and create a membrane effect that limits vertical settlement.

4.4. Economic analysis

From a perspective of overall optimisation, the economic criterion stands out as the key factor for assessing the suitability of a road solution. The comparative cost estimate shown in Table 3 highlights the initial additional cost associated with incorporating a geogrid.

The initial additional cost is 3.25% for the construction of a road surface using geogrids. Furthermore, other studies indicate an additional cost of around 3–5% for geosynthetic road reinforcement [2].

The discussion assesses the scope of this solution in terms of the financial, environmental and operational benefits it generates over the entire life cycle. This additional cost must be weighed against the long-term savings. Indeed, this additional cost (3.25%) remains modest when compared to: less material requiring maintenance, fewer repairs due to rutting, and greater durability (an additional 5 years according to the manufacturer Huesker). Indeed, the technical benefits (less settlement/rutting) result in a longer period without the need for intervention. These observations are consistent with recent studies [13], which reported an improvement in the durability of unpaved pavements reinforced with geogrids in a humid tropical climate.

The use of geosynthetics therefore helps to reduce subsequent maintenance costs. This assessment therefore appears generally positive, especially in contexts where durability is critical (sensitive soils, high maintenance costs). As noted in the literature, 'the use of a geosynthetic allows for optimisation of design, a reduction in maintenance costs, and a significant improvement in pavement durability" [2]. Our study qualitatively confirms this economic trend. The financial results presented should be interpreted as indicative; a comprehensive life-cycle cost analysis with detailed assumptions and long-term scenarios is proposed as a priority extension of this work.

Although the main objective of this work was to conduct a technical and financial analysis of the incorporation of a geogrid into the pavement structure, it is worth highlighting the positive environmental benefits associated with this solution. Indeed, the reduction in the thickness of the granular layers made possible by the reinforcement leads to a significant decrease in the volumes of materials extracted and transported, thereby limiting greenhouse gas emissions associated with quarrying and logistics activities. Furthermore, the use of geosynthetics—long-lasting polymeric products—helps to extend the intervals between maintenance works and reduce the overall ecological footprint of the infrastructure's life cycle. In tropical contexts, where lateritic and clay soils are widely used, the use of geogrids improves the durability of road pavements without the systematic use of chemical stabilisers (lime, cement), thereby avoiding potential impacts on soil and groundwater quality. The integration of geosynthetics into road design is therefore part of a sustainable development approach, balancing mechanical efficiency, economic viability and environmental responsibility.

5. Conclusion

This comparative study highlights that the integration of a geosynthetic (geogrid) into the sub-base layer of a flexible pavement significantly strengthens the structure. Numerical simulations showed a notable reduction in deformations under load (estimated gain ≈ 20%), justifying a modulus improvement factor for the sub-base layer of around 1.2. This mechanical gain results in a reduction in the required base thickness (from 30 cm to 20 cm in our case), thus leading to a more cost-effective structural design.

The financial analysis shows that a slight initial cost overrun (3.25%) due to the supply of the geogrid is offset by the technical benefits: optimised design, reduced volume of materials, and, above all, lower future maintenance costs thanks to increased durability. These results confirm the conclusion that 'the integration of geosynthetics for the reinforcement of road infrastructure presents significant technical and economic benefits' [2,3], particularly in African contexts where the stability of roadbeds on sensitive soils is crucial.

It should be noted, however, that exact performance depends on the quality of installation (proper compaction around the geogrid, absence of liners, etc.), the strength of the geosynthetic (tensile modulus) and, the soil-geosynthetic interaction (frictional interface). Our simplified numerical approach (elastic materials, static simulation) does not account for the viscoelasticity of asphalt or the actual dynamic effects of traffic. Nevertheless, it captures the overall effect of the geosynthetic on stiffness. The extrapolation of the results to real-world conditions remains favourable, as evidenced by several real-world cases where the observed gain was similar to our estimate.

Looking ahead, this study encourages the wider use of geosynthetics in tropical road projects. Further research could refine the design (advanced models, asphalt fatigue, non-linear soil behaviour) and evaluate long-term performance data. Nevertheless, for the case study of the Boucle de la Lekié, the proposed approach has already demonstrated its effectiveness.

Acknowledgement

The authors wish to express their sincere gratitude to the National Advanced School of Public Works (ENSTP), Yaoundé, for its academic guidance and technical support throughout the course of this research.

They also extend their thanks to the engineers and project managers involved in the rehabilitation of the Lekié Loop, whose collaboration was essential for data collection and pavement performance analysis.

Finally, the authors dedicate this work to all engineers and development professionals who contribute daily to building sustainable, resilient, and context-adapted road infrastructures in tropical environments.

Declarations

The authors declare that this manuscript is original, has not been published previously, and is not under consideration for publication elsewhere. All authors have made a significant contribution to the conception, execution, and writing of this work and have approved the final version of the manuscript.

Funding

This research did not receive any specific grant from funding agencies in the public, commercial, or not-for-profit sectors. The study is based on independent numerical modelling and scientific analysis conducted by the authors.

Conflicts of interest

The authors declare that they have no conflicts of interest relating to the publication of this paper.

Authors' contributions

Fongang Kamgaing Giovanni Paolo designed the study, carried out all numerical modelling (Alizé-Lcpc and Plaxis 3D), interpreted the technical results, and drafted the manuscript. Charles Bwemba supervised the research, facilitated access to field data, and contributed to the critical review of the manuscript. Laurent Sakou validated the numerical models, refined the simulations, and took part in the comparative economic analysis of the pavement structures.

All authors have read and approved the final version of the manuscript.

Technical appendices

Appendix A – Notations and abbreviations.

All variables are defined in a single location (Appendix Notations). E-moduli in MPa, geogrid stiffnesses in kN/m, displacements in mm, strains ε in mm/mm (or %).

- A_s: Area of the load circle

- BB: Bituminous concrete

- C: Soil cohesion (kPa)

- CBR: California Bearing Ratio, soil bearing capacity index (%)

- E: Modulus of elasticity (Young's modulus) of the material (MPa)

- EA: Axial stiffness of the geogrid (kN/m)

- $E_{initial}$: Initial effective modulus of elasticity before reinforcement (MPa)

- E_{final}: Effective modulus of elasticity after reinforcement (MPa)

- F_c: Chemical attack and ageing factor (≈ 1.15 – 1.30)

- F_{cr}: Creep factor, a function of service life (≈ 1.25 – 3.0)

- F_i: Damage factor at installation (≈ 1.10)

- F_m: Manufacturing factor (≈1.00)

- F_s: Overall safety factor

- F_o: Force or point load (kN)

- GLAR: Lateritic gravel

- GNT: Untreated Gravel

- G_0: Modulus of stiffness at very small strains (Hardening Soil model) (MPa)

- k: Modulus improvement factor for the sub-base layer (dimensionless)

- k': Primary improvement coefficient (dimensionless) calculated in relation to deformations or moduli

- NMB: Primary improvement coefficient (dimensionless) calculated in relation to strains or moduli

- PST: Platform / subgrade (designation of the underlying soil)

- σ: Stress (MPa)

- ν (nu): Poisson's ratio (dimensionless)

- **ε**: Strain (dimensionless; mm/mm or %)

- Ux, Uy, Uz: Nodal displacement components (mm or m); Ux = Uy = Uz = 0 indicates fixed support

- %: Percentage

Appendix B – Main equations used.

Hooke's linear relationship for an isotropic elastic material is written as:

$$\sigma = E \times \varepsilon \qquad \text{(Eq. B3)}$$

Where σ is the stress, ε is the strain, and E is the modulus of elasticity. In the small-displacement approximation, the deflection resulting from a given load is inversely proportional to the material's modulus of elasticity E. Thus, for two models simulating the same geometry with different values of E, we can estimate:

$$k = \frac{E_{final}}{E_{initial}} \approx \frac{\varepsilon_{initiale}}{\varepsilon_{final}} \qquad \text{(Eq. B5)}$$

Appendix C – Geosynthetic parameters.

After consulting the COST ACTION (2008) tables [7], the geosynthetic selected for the reinforcement of pavement structures is the Basetrac*Duo-C PET 40-35 B15 geogrid (Figure 6).

The Basetrac*Duo-C PET 40-35 B15 geosynthetic is an 'all-in-one' geocomposite combining a high-tenacity biaxial polyester (PET) geogrid and a non-woven polypropylene (PP) geotextile. It has a weight per unit area of 410 g/m² and a nominal tensile strength of 60 kN/m. Thanks to its protective polymer coating and heat-sealed construction, it simultaneously reinforces the sub-base, separates the retaining wall from the lateritic gravel, and provides vertical filtration and drainage. Its large mesh size (35 x 35 mm²) allows it to interlock perfectly with the local lateritic gravel, ensuring uniform stress distribution.

Geogrids used in roads typically have tensile moduli ranging from 500 MPa to 2000 MPa, depending on the type. For example, a PP30/30 geogrid has a linear modulus of ≈1000 MPa [4]. They are laid with minimal curvature in the granular layers, with a minimum overlap of approximately 0.5 m at the joints to ensure the integrity of the reinforcement.

Appendix D – PLAXIS procedure (extract).

1. Define the 3D geometric model of the layers and assign boundary conditions to the model (dimensions, thicknesses, soil zones).

2. Assign the mechanical properties (soil behaviour models, modulus of elasticity E, Poisson's ratio ν).

3. Create a suitable mesh (tetrahedral elements).

4. Apply the surface load in accordance with the French standard axle (distributed pressure).

5. Configure the calculation phases.

6. Run the calculation for the different stages, then extract the displacements δ.

Appendix E – Calculation plan for the bill of quantities.

Figure 2 illustrates the typical cross-section. The asphalt carriageway is a two-lane, two-way road, with a width of 3.5 m × 2. The stabilised verge, meanwhile, extends 1.5 m on either side of the carriageway, giving a total width of 10 m for the road platform.

To draw up the bill of quantities for the road surface and verges, we first use the typical cross-section of the section to determine the widths and areas to be covered.

The structural cross-section (Figure 7), which describes the sequence of layers (sub-base, foundation + base, and surface course) with their projected thicknesses, then allows these areas to be converted into volumes by multiplying the area of each strip by the corresponding thickness.

The gross volumes thus obtained are adjusted using mass-to-volume conversion factors based on in-situ densities.

Unit prices from the 2025 Price List of the Ministry of Trade of the Republic of Cameroon are applied, supplemented by the company's internal price schedules to account for local and contractual specifics. The overall costs of the 'without geosynthetics' and 'with geosynthetics' variants were calculated by re-adjusting the adjustment coefficients relating to overheads and technical contingencies. The supplementary calculations confirm the order of magnitude of the improvements and costs discussed in the main body of the article.

List of tables

Table 1. Design verification of the contract pavement (thicknesses, moduli, allowable values and calculated values of µdef; maximum deflection)

Traffic Class	Type of materials	Thickness (cm)	Modulus (MPa)	Permissible values (µ def)	Calculated values (µ def)	Verification	Maximum deflection
Traffic T2	Wearing course (BB)	05	3245	158.1	229.0	Unsatisfactory	61.8
	Base layer / foundation (GNT)	20	400	540.3	1040.2	Unsatisfactory	
	Scarification + material addition (GLAR)	30	150	540.3	837.8	Unsatisfactory	
	Ground level (S3)	Infinite	100	540.3	484.4	Satisfactory	

Table 2. Design verification of the geogrid-reinforced pavement (modified thicknesses, moduli, allowable values and calculated values of µdef; maximum deflection)

Traffic Class	Type of materials	Thickness (cm)	Modulus (MPa)	Valid values (µ def)	Calculated values (µ def)	Verification	Maximum deflection
Traffic T2	Wearing course (BB)	05	3245	158.1	226.8	Unsatisfactory	61.2
	Base layer / foundation (GNT)	20	400	540.3	1040.2	Unsatisfactory	
	Scarification + material addition (GLAR)	20	180	540.3	735.6	Unsatisfactory	
	Ground level (S3)	Infinite	100	540.3	613.2	Unsatisfactory	

Table 3. Detailed comparative estimate of construction costs — Initial pavement vs Reinforced pavement (units, quantities, unit prices, totals excluding VAT and including VAT)

Pavement Estimate - Section 2								
				Initial road surface			**Reinforced road surface**	
Trade: 300 – Road surface and verge								
Price no.	Description	Unit	Unit price (FCFA)	Gross quantity	Total price (FCFA)		Gross quantity	Total price (FCFA)
310	**Form layer**							
312	Scarification, recycling and general rehabilitation of the base course	m^3	1,885	104,296	196,597,960		52,148	98,298,980
	Supply and installation of Base Trac Duo-C geogrid	m^2	2,500	-	-		263,700	659,250,000
313	Supply of lateritic gravel from a borrow pit in Couche de forme	m^3	4,896	23,220	113,685,120		13,061	63,947,880
320	**Verge and pavements**							
322	Sand-blasted impregnation	m^2	1,558	178,767	278,518,986		178,767	278,518,986
323	Two-coat render on verge	m^2	3,962	178,767	708,274,854		178,767	708,274,854
330	**Road construction**							
332	Base course/sub-base of crushed stone 0/31.5 (20 cm)	m^3	39,010	31,513	1,229,322,130		23,635	921,991,598
335	Primer	m^2	766	263,700	201,994,200		263,700	201,994,200
337	Asphalt concrete surfacing (5 cm)	m^2	13,415	263,700	3,537,535,500		263,700	3,537,535,500
	Total excluding VAT				6,265,928,750			6,469,811,998
	VAT	19.25%			1,206,191,284			1,245,438,810
	Total incl. VAT				**7,472,120,034**			**7,715,250,807**

List of figures

Figure 1. Results of geotechnical identification tests (granulometric analysis and Atterberg limits) and characterisation tests (Proctor and CBR tests) on (a) PST (b) Sub-base

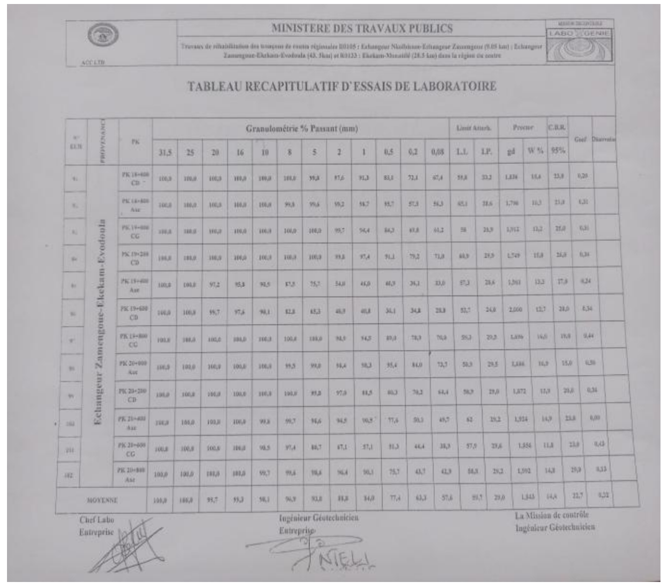

(a)

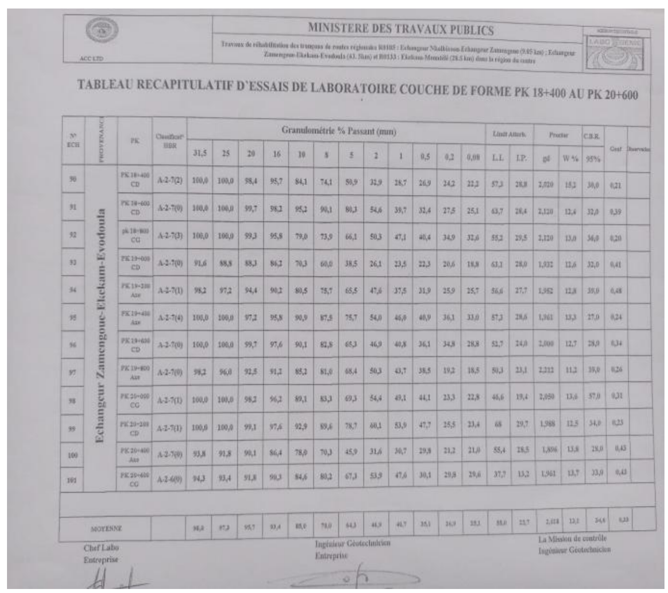

(b)

Figure 2. Typical cross-section of the Boucle de la Lekié (platform geometry, verges and carriageway widths)

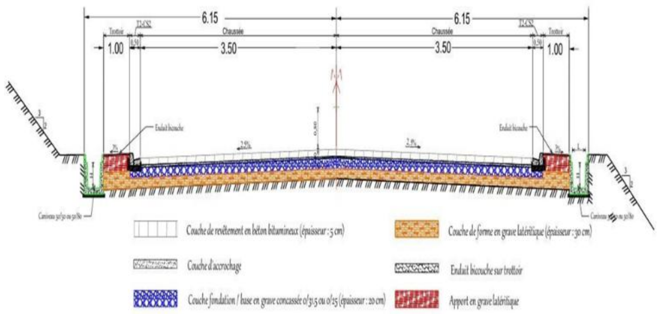

Figure 3. PLAXIS 3D three-dimensional model of the reinforced pavement (layer sequence, geogrid placement and boundary conditions)

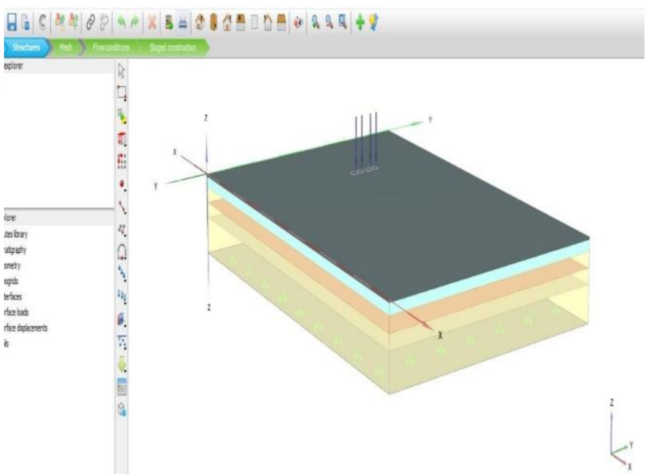

Figure 4. Maximum deformation of the pavement grid under a 130 kN axle load (a) Standard pavement (b) Pavement reinforced with a geogrid

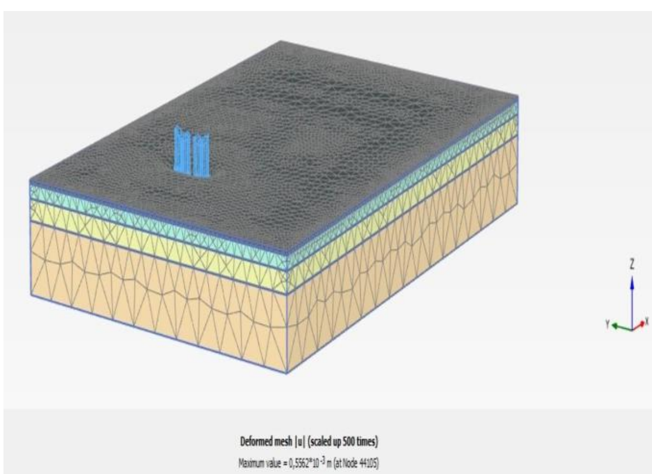

(a)

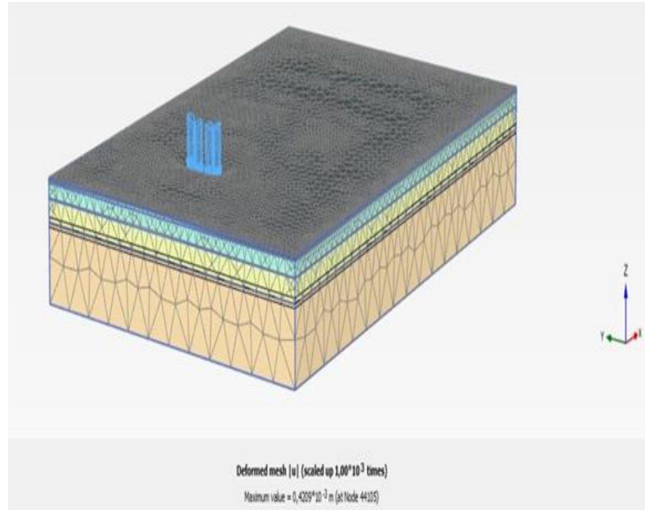

(b)

Figure 5. Variation in deflection as a function of sub-base thickness

(Alizé-LCPC results for variants)

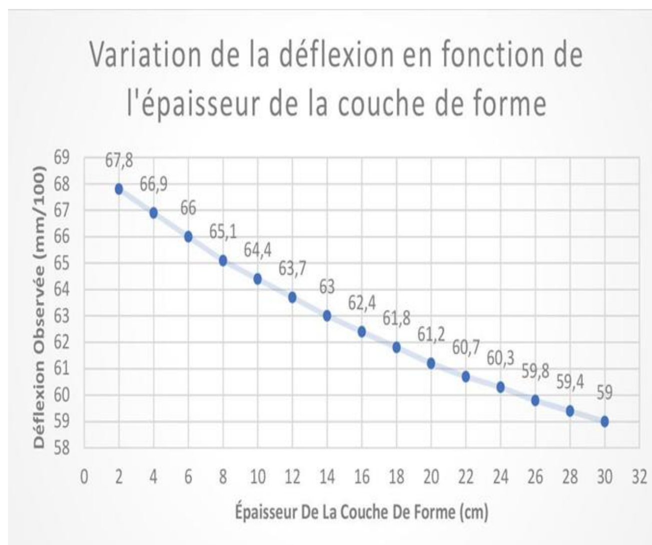

Figure 6. Construction details and technical characteristics of the Basetrac*Duo-C PET 40-35 B15 geogrid

(surface mass, tensile strength, mesh dimensions)

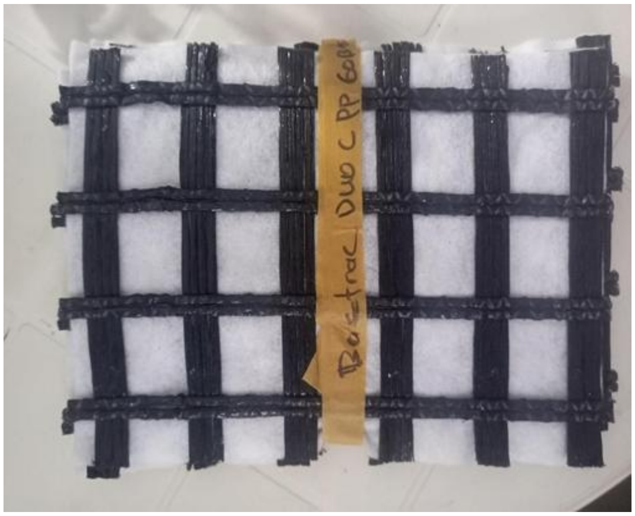

Figure 7. Structural cross-section of the reinforced pavement (layers: asphalt, base + sub-base, sub-grade, sub-soil)

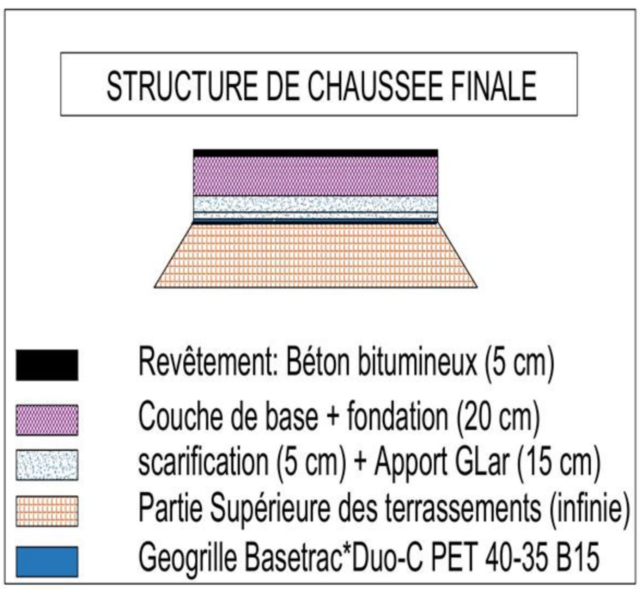

References

[1] Tribune de l'Info, Rehabilitation of the Lekié Loop: a new lease of life for the works on the three sections, Tribune de l'Info (2023), https://tribunedelinfo.com/rehabilitation-de-la-boucle-de-la-lekie-un-souffle-nouveau-sur-les-travaux-des-trois-sections/, accessed 20 October 2025.

[2] International Geosynthetics Society (IGS), Geosynthetics in Unpaved Roads (French version), IGS Educational Series, (2022), https://library.geosyntheticssociety.org/wp-content/uploads/resources/educational-documents/Unpaved%20Roads/French.pdf, accessed 20 October 2025.

[3] A. Watn, Geosynthetics: technical aspects and applications in civil engineering, in Rencontres Géosynthétiques 2011, French Geosynthetics Committee (CFG), Paris, France (2011) 47–62, https://www.cfg.asso.fr/sites/default/files/files/cd-rom-2011/047-062.pdf.

[4] Tensar International, Flexible Pavement: Layers, Components, and Advantages, Technical Article, Tensar International (2020), https://www.tensarinternational.com/resources/articles/what-are-the-function-of-layers-in-a-flexible-pavement, accessed 20 October 2025.

[5] Alizé-LCPC, Software for the design of pavement structures, LCPC Software Documentation (2024), https://www.alize-lcpc.com/fr/.

[6] T. Chazallon, Modelling of viscoelastic pavements, ResearchGate Publications (2013), https://www.researchgate.net/publication/258075395_Modelisation_de_chaussees_viscoelastiques.

[7] COST Action 348, Reinforcement of Pavements with Steel Meshes and Geosynthetics – Final Report of the COST Action 348, European Cooperation in Science and Technology (COST), Brussels, Belgium (2008) 242 p.

[8] Comité Français des Géosynthétiques (CFG), Geosynthetics: definition, typology and applications, CFG Publications, Paris (2021), https://www.cfg.asso.fr/les-geosynthetiques.

[9] Bentley Systems, PLAXIS 3D: Geotechnical Engineering Software, Bentley Systems Inc., Exton, PA, USA (2024), https://www.bentley.com/software/plaxis-3d/.

[10] A. F. Abiola, K. A. Alhassan, Performance evaluation of geogrid-reinforced lateritic pavements in tropical regions, Constr. Build. Mater. 280 (2021) 122–139.

[11] M. R. Islam, L. Zhang, Geosynthetics in sustainable pavement design for developing countries, Transp. Geotech. 37 (2022) 100–112.

[12] E. K. Owusu, P. E. Amoako, Behaviour of reinforced subgrade soils under cyclic loading: A numerical study, Int. J. Pavement Eng. (2023), https://doi.org/10.1080/10298436.2023.2174956.

[13] L. D. Ndlovu, J. S. Maina, Experimental assessment of geogrid-stabilised unpaved roads under tropical climate, Int. J. Geosynth. Ground Eng. 11 (2) (2024) 85–98.